J Fluoresc (2011) 21:423–432
DOI 10.1007/s10895-010-0731-0

ORIGINAL PAPER

Gd^{3+} Sensitized Enhanced Green Luminescence in Gd: $Tb(Sal)_3Phen$ Complex in PVA

Gagandeep Kaur · Y. Dwivedi · S. B. Rai

Received: 23 April 2010 / Accepted: 28 September 2010 / Published online: 8 October 2010

Abstract Ternary and tertiary complexes of $Tb(Sal)_3Phen$ and $Gd:Tb(Sal)_3Phen$ were synthesized and characterized in PVA polymer. The structural properties of these systems were evaluated on the basis of NMR and FT-IR techniques. The absorption, excitation and emissive properties of the Tb^{3+} ion were improved when coordinated with Sal and Phen ligands. Photoluminescence properties of the complexes in solution, crystals and dispersed in PVA film were explored in steady state and in time domain. Selective excitations (487, 355, 310 and 266 nm) of Tb^{3+}, Sal and Gd^{3+} ions reveal an intramolecular energy transfer process. The emission of $Gd:Tb(Sal)_3Phen$ complex in PVA indicates the contribution of Gd^{3+} ion to enhance the emission intensity of Tb^{3+} ion. On the basis of these investigations, photophysics was widely discussed in terms of energy transfer and encapsulation effect.

Keywords Lanthanide complex · Energy transfer · Aromatic carboxylic acid · Salicylic acid · 1, 10-Phenanthroline · Antenna ligand · Fluorescence enhancement

PACs No. -95.75.Fg · 87.64.k- · 78.47.Jc · 64.70. Km · 33.50.-J · 68.35.bm

Introduction

Considering the interesting photophysical properties of organic-lanthanide ion coordinated complexes, these materials are suitable for numerous applications in electroluminescent and photoluminescence devices, novel optical displays, detectors, telecommunications and also used in biological probing etc. They have the striking advantages of stability, cost-effectiveness, ecologically acceptability and bulk manufacturing [1]. When these complexes are dispersed in polymers, these complexes simultaneously bear the advantage of sharp enhanced emission bands of rare earth ions and the flexibility of shape and size of polymer.

Complexation of lanthanide ions (Ln^{3+}) with organic ligands (β-diketone and corboxylate) provide an extra stability to the molecular structure, sheath to Ln^{3+} ions from higher lattice vibrations and an efficient sensitization for Ln^{3+} which intensifies the luminescence intensity [2, 3]. These organic ligands predominantly absorb the UV/blue radiations and subsequently yield strong emission in visible region. When organic ligand and the Ln^{3+} ions are in same coordination sphere, efficient energy transfer from ligand to Ln^{3+} ions is facilitated. However, the energy gap between the excited triplet level of the organic ligand and the lowest excited energy level of the Ln^{3+} ion is a crucial factor in the transfer of energy among them [4]. The organic sensitization of Ln^{3+} ions has been studied extensively for its opportunities in LED applications and laser systems.

Most of such studies were focused on Tb^{3+} and Eu^{3+} ions as these ions possess large yield in green and red regions respectively and are suitable for fluoroimmunoassays, DNA and RNA labelling and structural probes [5]. The large energy gap between excited and lower states of these ions facilitates the radiative relaxation process. These ions could effectively be sensitized by Salicylic acid as it posses large quantum yield in the blue region (400–500 nm). Salicylic acid is one of the few ligands which serve simultaneously the advantage of chelation as well as sensitization to the Ln^{3+} ions. These emissions could

G. Kaur · Y. Dwivedi · S. B. Rai (✉)
Laser and Spectroscopy Laboratory, Department of Physics,
Banaras Hindu University,
Varanasi, India 221005
e-mail: sbrai49@yahoo.co.in

further be improved by introducing neutral Ln^{3+} ions in complex viz. Lu, Y, La and Gd ions.

Li et al. reported the fluorescence enhancement via inter and intramolecular energy transfer in Tb-ATP-phen system by introducing Gd^{3+} ion [6]. Wang et al. studied the coordinated blend of active (Eu, Tb) rare earth ions and an inert (La, Y, Gd) rare earth ion with the organic- inorganic hybrid materials and reported the luminescence enhancement effect for inert rare earth ions [7]. Jiao et al. reported the sensitizing influence of Sc, La, Gd, Lu on the luminescence properties of green phosphorY_2SiO_5:Ce:Tb under excitation by cathode rays and 355 nm UV light [8].

Present work is focused on detail investigations regarding structural and optical properties of $Tb(Sal)_3Phen$ and $Gd:Tb(Sal)_3Phen$ complexes in solution, crystalline form and dispersed in polyvinyl alcohol (PVA) films. The characteristic green luminescence of Tb^{3+} ion is found to improve on UV/blue excitations in these complexes. Luminescence enhancement in Tb^{3+} is explained in terms of energy transfer processes through Sal→Tb and in latter case both Sal→Tb and Gd→Tb channels.

Experimental

Ln compounds (Gadolinium oxide, Terbium oxide) and the Salicylic acid used are 99.9% pure while 1,10-phenanthroline is of 99.5%. These compounds alongwith polyvinyl alcohol (PVA, mw. 14000) were purchased from Sigma Aldrich and used without further purification. Standard stock solutions (0.01 M) of Ln^{3+} were prepared by dissolving a known amount of oxides (Gd_2O_3 and Tb_4O_7) in hydrochloric acid. The complexes of organic-lanthanide ion were prepared by mixing the ethanolic solution of Salicylic acid (Sal) (2.3 wt%) and 1,10-phenanthroline (Phen) (0.56 wt%) to the previously prepared solution (0.01 $molL^{-1}$) of gadolinium chloride and terbium chloride in 3:1:1 ratio. Phen was mixed to the complex for extra rigidity to molecular structure. Mixture thus prepared was evaporated to dryness at room temperature over a course of time in air. White and brownish crystals of $Gd(Sal)_3Phen$ and $Gd:Tb(Sal)_3Phen$ complexes were collected respectively. The ethanolic solution of as prepared complex was mixed with the solution of PVA polymer in distilled water. It was stirred rigorously for half an hour in air to get homogenous, transparent viscous solution which was then poured in the petri dish to dry overnight in computerized furnace at a 50°C temperature for removal of excess solvent to get film of uniform thickness (0.2 mm). These films were stored in humidity free atmosphere, for further optical measurements.

The absorption spectra was recorded using a Cary 2390 double beam UV–vis spectrophotometer in the wavelength range 200–500 nm. Fourier Transform Infra-Red (FTIR) spectra were recorded using Spectrum RX-I spectrophotometer (Perkin Elmer) and NMR spectra using FTNMR-JOEL AL300 system at 80 Hz. For emission and excitation spectra, a Spectrofluorometer [Flouromax–4, Horiba Jobin Yvon] was used. The dynamics of luminescence were examined using the third harmonic of pulsed Nd:YAG laser [Spitlight–600, Innolas, Germany] having pulse width 7 ns, as an excitation source. The overall response time of our detection system was < 1 μs. The collected signal was fed to 150 MHz digital oscilloscope (model no. HM 1507, Hameg Instruments) to record the decay curve. Lifetime of the radiative levels was estimated by fitting the decay curve in an exponential function. The detector offset was removed before fitting and the data were normalized to the initial voltage.

Results and Discussion

Structural Analysis

UV–vis absorption spectra of PVA and Ln^{3+} (Gd^{3+} and Tb^{3+} ion) coordinated complexes of Sal/Phen doped in PVA films were recorded in the range of 190–600 nm under identical conditions [see Fig. 1]. The absorption spectrum of PVA film contains strong characteristic bands at 195 nm and a weak band at 275 nm. These bands are assigned as π→π* electronic transition of PVA molecule. On addition of $GdCl_3$ and $TbCl_3$ salt in PVA films, it is very difficult to assign the inter-configurational transitions of Gd^{3+} and Tb^{3+} ions as these get buried in the broad background of PVA. Even taking PVA absorption in

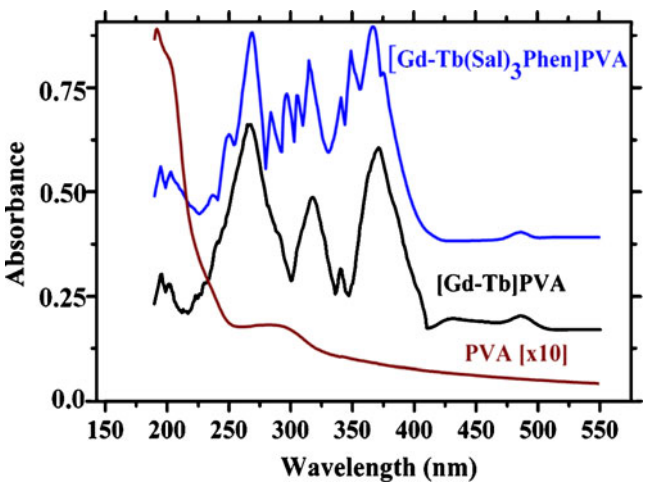

Fig. 1 Absorption spectra of undoped PVA and [Gd-Tb], $Gd_{1.0}$-$Tb_{1.0}(Sal)_3Phen$ doped PVA films. Spectra of [Gd-Tb] and Gd-Tb $(Sal)_3Phen$ doped PVA films were taken keeping PVA in background

reference, only a few weak bands at 269, 315, 341, 367 and 486 nm corresponding to the electronic transitions from ground state $^7F_6$ to different excited states $^5I_5$, $^5H_7$, $^5L_6$, $^5L_{10}$ and $^5D_4$ levels of Tb^{3+} respectively were recognized.

UV–vis absorption spectrum of the Gd:Tb(Sal)$_3$Phen complex doped PVA film consist of bands at 238 nm and 305 nm corresponding to $S_2 \leftarrow S_0$ and $S_1 \leftarrow S_0$ transitions of Sal superimposed to the low intensity broad PVA absorption bands. A broad band at 268 nm is basically composed of $^6D_j \leftarrow ^8S_{7/2}$ transition of Gd^{3+} ion, $\pi^* \leftarrow \pi$ transition of the aromatic ring of Phen and $^5I_5 \leftarrow ^7F_6$ transition of Tb^{3+} ions. The absorption bands of Tb^{3+} ions are observed to be improved in intensity and resolved. Few new bands at 284, 297, 305, 351 and 376 nm corresponding to $^5I_8$, $^5H_5$, $^5H_6$, $^5L_9$, $^5G_6 \leftarrow ^7F_6$ transitions also appear along with the bands observed in Gd-Tb ions in PVA film without Sal/Phen. The enhancement in the extinction is due to the organic-lanthanide coordination and consequently due to the encapsulation effect. The coordination of Ln^{3+} ion with the Sal/Phen complex prevents the interactions of Ln^{3+} ions from the vibrations of the host molecules, which improves the transition probability of the transitions.

The infrared absorption spectra of salicylic acid, 1,10-phenanthroline and Tb(Sal)$_3$Phen complex are recorded in the range of 400–4000 cm^{-1} and the different vibrations were assigned [Fig. 2]. The FT-IR spectra displays the expected strong characteristic absorptions of the salicylic acid $\upsilon_{Ar\text{-}OH}$ (1295 cm^{-1}), $\delta_{O\text{-}H}$ (1485 cm^{-1}), $\upsilon_{C=O}$ (1665 cm^{-1}), υ_{OH} (COOH, 2597 cm^{-1}), υ_{OH}^{COOH} (intermolecular H-bond, 2856 cm^{-1}) and υ_{OH}^{COOH} (intramolecular H-bond, 3237 cm^{-1}). The characteristic absorption bands of C=O and C-O belonging to the carboxylic acid ligands disappear, while the characteristic absorption peaks of carboxylic group COO^- appear in the IR spectra of the complex when compared with Sal. Moreover, $\upsilon_{Ar\text{-}OH}$ stretching vibration shifts to lower energy which suggests that the oxygen atoms of carbonyl group of conjugated carboxylate group was coordinated to Ln^{3+} ions through the oxygen [9]. The vibrational frequencies of the characteristic absorptions $\delta_{(C\text{-}H)}$ (733 and 850 cm^{-1}), $\upsilon_{C=O}$ (1507, 1589, and 1619 cm^{-1}) and $\upsilon_{C=N}$ (1647 cm^{-1}) were assigned in phenanthroline. Evidence of chemical bond formation between Ln^{3+} ions and the nitrogen atoms observed as the benzene ring $\delta_{(C\text{-}H)}$ bending vibration were shifted to lower frequencies and the C=N vibration was vanished [10].

^1H and ^{13}C NMR spectra were recorded for the samples in standard DMSO solution, for detailed structural investigation. Figure 3 represents the comparison of ^1H-NMR spectrum of free salicylic acid, 1,10-phenanthroline and Tb(Sal)$_3$Phen complex. Phenanthroline and salicylic acid molecules contained 8 and four equivalent protons respectively. Peaks corresponding to Ar-H are shifted downfield in case of Tb coordinated complex. Further peaks due to –COOH and –OH of salicylic acid observed at 13.4 and 11.3 disappear in Tb(Sal)$_3$Phen complex, which shows the coordination of Tb^{3+} ions with the carbonyl group of salicylic acid thus the aromatic hydrogen causing downfield shift. The substantial changes in the peak positions observed are due to complexation of Ln^{3+} ions. The shift is due to electron-spin relaxation time and magnetic anisotropy of Tb^{3+} ion [11, 12]. The chemical shifts observed in ^{13}C NMR spectra of phenanthroline and the complex shows that both nitrogen atoms of phenanthroline were coordinated in the coordination compounds [13].

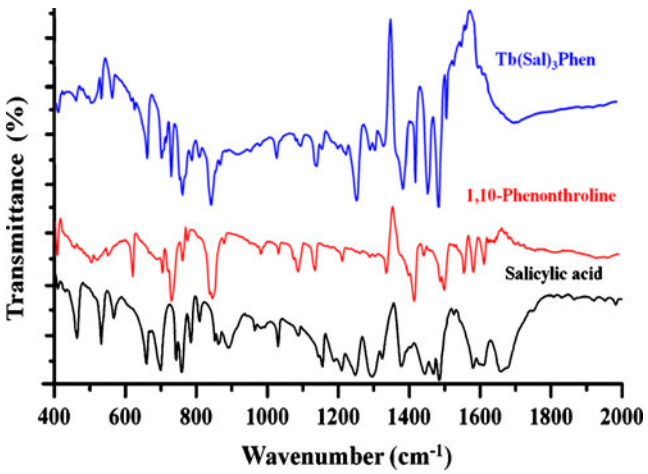

Fig. 2 FTIR spectra of Salicylic acid, 1, 10 Phenanthroline and Tb (Sal)$_3$Phen complex

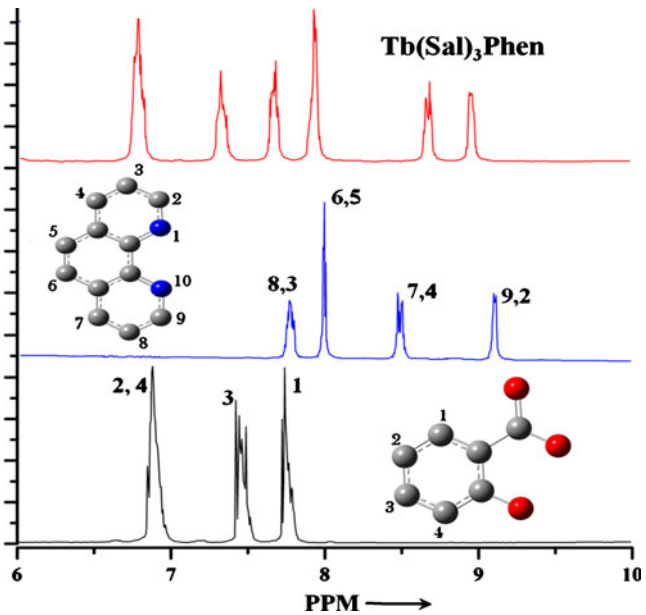

Fig. 3 ^1H-NMR spectra of Salicylic acid, 1, 10 Phenanthroline and Tb(Sal)$_3$Phen in DMSO solution

Excitation Spectra

The excitation spectra of $Tb(Sal)_3Phen$ and $Gd:Tb(Sal)_3$-Phen complex in PVA films corresponding to $^5D_4 \rightarrow {}^7F_5$ (544 nm) transition of Tb^{3+} ion were recorded to confirm the possibility of energy transfer from salicylate ligand to Tb^{3+} ions and shown in Fig. 4.

The excitation spectrum of $TbCl_3$:PVA sample shows few weak bands at 341, 351, 358, 369 and 377 nm wavelengths corresponding to excited state absorption of Tb^{3+} ion. The excitation spectrum of $Tb(Sal)_3Phen$ complex was largely dominated by the ligand bands, pointing to a efficient antenna effect. Spectrum shows a weak band at 240 nm and broad band from 270 to 387 nm. A comparison of absorption spectrum of Sal/Phen complex in PVA with excitation spectrum of $Tb(Sal)_3Phen$ complex reveal a considerable overlap between the absorption of salicylate ligand ($\pi \rightarrow \pi^*$) and absorption in excitation spectrum. It is interesting to note that on addition of Gd^{3+} in $Tb(Sal)_3Phen$ complex, the extinction intensity was observed to improve further. The integrated excitation energy in the range of 230–387 nm for $^5D_4 \rightarrow {}^7F_5$ transition in $Gd:Tb(Sal)_3Phen$ complex is found to be 10 times higher than $Tb(Sal)_3Phen$ complex. The improvement observed is due to the fact that electron conjugated system of the complexes is much larger than that of the free-base Sal and has a higher molar absorptivity [14].

An asymmetric excitation broad band (280–360 nm) centered at 338 nm appears due to the $n \rightarrow \pi^*$ transition of salicylate ligand. The appearance of the bands corresponding to the Tb^{3+} ion emission clearly indicate the effective sensitization for Tb^{3+} ions by salicylate ligand through $\pi \rightarrow \pi^*$ and $n \rightarrow \pi^*$ transitions as well. This reveals that the organic ligands are within coordination sphere of the Ln^{3+} ions and could effectively sensitize them.

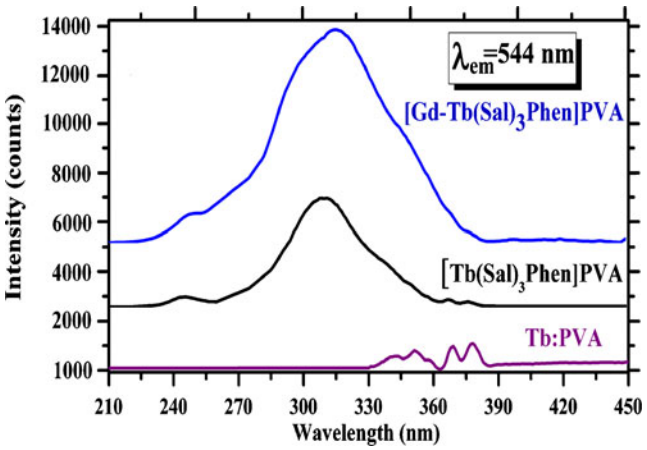

Fig. 4 Excitation spectra of $TbCl_3$, $Tb(Sal)_3Phen$ and $Gd:Tb(Sal)_3Phen$ complex in PVA corresponding to $^5D_4 \rightarrow {}^7F_5$ (544 nm) transition of Tb^{3+} ion

Photoluminescence on 487 nm Excitation

The photoluminescence spectra of $TbCl_3$, $Tb(Sal)_3Phen$ and $Gd:Tb(Sal)_3Phen$ complexes doped in PVA film were recorded using 487 nm radiation as an excitation source [Fig. 5]. The PVA film doped with these complexes exhibits characteristic emission peaks at 487, 544, 583 and 618 nm of Tb^{3+} ions emanating from $^5D_4 \rightarrow {}^7F_j$ (j=6, 5, 4, 3) transitions respectively and among them $^5D_4 \rightarrow {}^7F_5$ transition (544 nm) is the brightest one. The luminescence intensity of Tb^{3+} ion was found to increase in $Tb(Sal)_3Phen$ complex as compared to $TbCl_3$ in PVA film, whereas it was reduced on addition of Gd^{3+} ions in the complex i.e. $Gd:Tb(Sal)_3Phen$.

The mechanism of observed transitions can be elucidated as: initially 487 nm (20534 cm^{-1}) photon was absorbed by Tb^{3+} and promoted to $^5D_4$ level. The radiative transitions from this level to different ground states are observed in luminescence spectrum. These emissions were found to improve in $Tb(Sal)_3Phen$ complex. Additionally, few new bands at 646 nm, 667 nm, and 679 nm attributed to the $^5D_4 \rightarrow {}^7F_j$ (j=2, 1, 0) are also observed. Though the intensity of the bands are noted to be improved in the $Tb(Sal)_3Phen$ complex doped PVA film the sensitization due to Sal/Phen complex is ruled out as both of the organic ligands do not absorb 487 nm radiation. The enhancement of the fluorescence is expected due to the encapsulation effect of Ln^{3+} ions, depending upon the ligand nature and the thermal stability of the complex. It appears that Tb^{3+} ions encapsulated in an organic cage of Sal/Phen complex get shielded from interactions of the matrix. Thus non-radiative relaxation via energetic phonons or hydroxyl group of the host is prohibited, which improves the radiative transition probability of the Ln^{3+} ions. Additionally, presence of Phen molecule in the complex strengthened the molecular structure and induces asymmetric coordination geometry around Tb^{3+} ions which assist hypersensitive radiative transitions [15].

The observed transitions though weaken in $Gd:Tb(Sal)_3Phen$ complex (Gd:Tb;1:1) as compared to $Tb(Sal)_3$-Phen, however it is still higher than $TbCl_3$ in PVA. In all these cases, Tb^{3+} ion concentration was fixed. The diverging result is due to the dilution of Tb^{3+} concentration on addition of Gd^{3+} ions as Tb-Tb separation increases.

Photoluminescence on 355 nm Excitation

The photoluminescence spectra of $TbCl_3$, $Tb(Sal)_3Phen$ and $Gd:Tb(Sal)_3Phen$ complexes doped in PVA film were recorded using 355 nm laser radiation and the resultant spectra were shown in Fig. 6. The 355 nm (~28170 cm^{-1}) laser photon partially resonate with $^5L_9$ level (~28490 cm^{-1}) of Tb^{3+} ion and $n \rightarrow \pi^*$ transition of salicylate ligand.

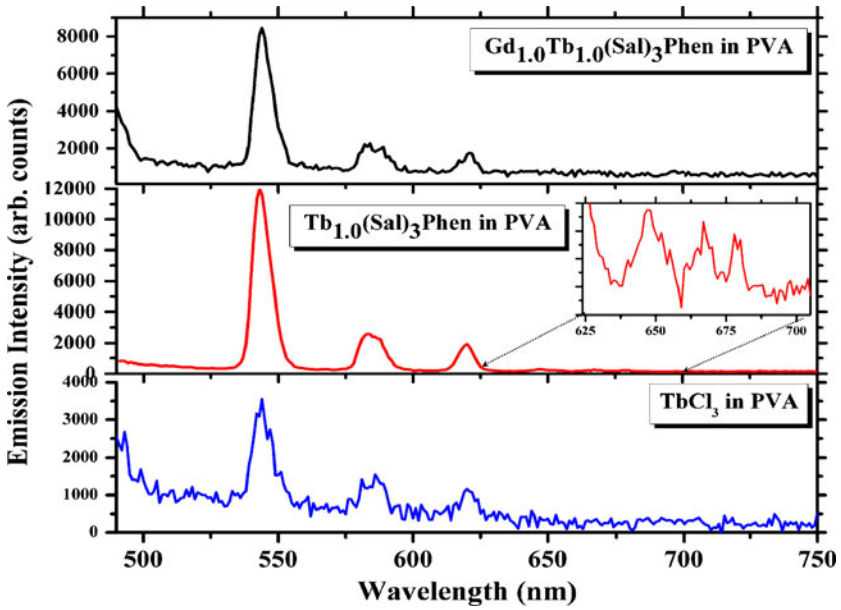

Fig. 5 Photoluminescence spectra of $TbCl_3$, $Tb(Sal)_3Phen$ and $Gd_{1.0}Tb_{1.0}(Sal)_3Phen$ complex doped PVA films on excitation with 487 nm radiation. Inset shows 6 times enlarged portion (625–705 nm) of Tb^{3+} transitions

However, Gd^{3+} ions could not be excited due to the large energy difference (~4088 cm^{-1}) of its next nearby energy level.

The characteristic emission peaks of $TbCl_3$ dispersed in PVA were observed as in previous case. The mechanism of observed transitions can be explained as: initially 355 nm (~28170 cm^{-1}) photon promotes Tb^{3+} ions to $^5L_9$ level. The excited Tb^{3+} ions relax non-radiatively from $^5L_9 \rightarrow {}^5D_3$ level. The emissions from $^5D_3$ level to lower lying states (^7F_i; i=3, 4, 5, and 6) are not visible, because the energy gap (~4500 cm^{-1}) between $^5D_3$ and $^5D_4$ levels is comparable to the highest lattice phonon vibrations of -OH, -NH, -CH, which induced rapid non-radiative relaxation. Further, the energy of $^5D_3 \rightarrow {}^7F_0$ and $^5D_4 \rightarrow {}^7F_6$ transition is analogous hence a possible cross relaxation process might also occur [16]. The possible pathway of the cross relaxation process is:

$$Tb^{3+}\left({}^5D_3\right) + Tb^{3+}\left({}^7F_6\right) \rightarrow Tb^{3+}\left({}^5D_4\right) + Tb^{3+}\left({}^7F_0\right)$$

Excited Tb^{3+} ions in $^5D_4$ level relax radiatively to different low lying levels [^7F_j; (j=6, 5, 4, 3)] and emit, observed colors.

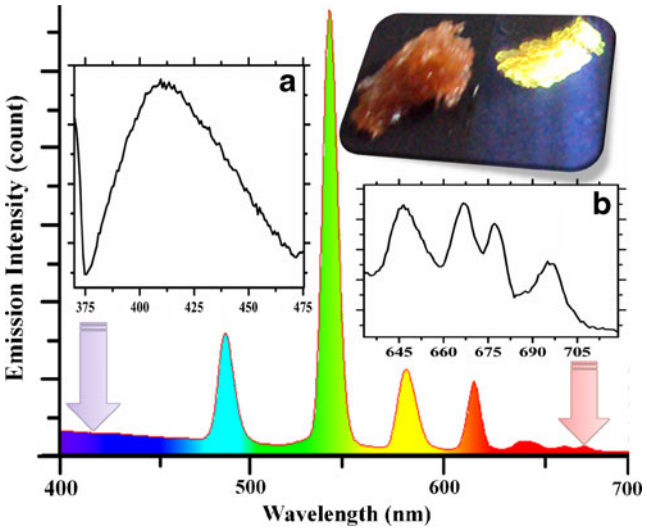

Fig. 6 Photoluminescence spectrum of $Tb(Sal)_3Phen$ complex doped in PVA on excitation with 355 nm. Inset [**a**] shows the emission of salicylate ligand at 415 nm and inset [**b**] shows the 40 times enlarged portion of (635–710 nm) spectrum showing Tb^{3+} transitions. Visual images of $Tb(Sal)_3Phen$ crystals with and without excitation of 355 nm laser is shown in inset (upper right)

When $Tb(Sal)_3Phen$ complex doped in PVA film was excited with 355 nm photon, it shows 40 fold enhancement in emission intensities of Tb^{3+} bands alongwith a broad band [370–475 nm] emission centered at 415 nm corresponding to salicylate ligand. A large increase in integrated emission intensity signifies an effective energy transfer from organic ligands to coordinated Tb^{3+} ion.

Generally aromatic carboxylate ligand adopts several coordination modes in complexes viz. bridging mode and bridging-chelating mode, through which the polynuclear complexes are formed [17–19]. For the effective energy transfer, Ln^{3+} energy level should coincide with the donor emissive level. Moreover, the lifetime of donor should not be too short to achieve an energy transfer nor too long to effectively populate the excited level. The mechanisms accountable for luminescence enhancement can be understood in the light of these. The earlier articles of Weller and others suggested an excited state intramolecular proton transfer from –OH group to C=O group of sal molecule [20–23]. Furthermore it's dimeric and the tautomeric forms emit in UV/blue regions which operate

as antenna ligand for Tb^{3+} ion. The 355 nm laser photon excites the unexcited sal to its singlet state (S_1). A part of this energy is lost through radiative channel to give a blue band and rest of the energy is lost through intersystem crossing to triplet state (T_1), which is transferred ultimately to the chelated active ion. The lowest triplet state of Sal and Phen lie at ~24184 cm^{-1} and ~22075 cm^{-1} [24] respectively and is suitable for sensitization to Tb^{3+} ion. Hence the long lived triplet states of organic compounds were effectively coupled with Tb^{3+} levels to transfer their energies to Tb^{3+} ions. We expect that the direct coordination of the Sal to Tb^{3+} ion improves the energy-transfer efficiency due to reduced donor-acceptor distance. The schematic energy level diagram explaining the luminescence process and the possible energy transfer pathways for the $Tb(Sal)_3Phen$ complex doped in PVA was shown in Fig. 7. The intramolecular energy transfer efficiency calculated is 76%, using the ratio of the peak area of donor [25]. On excitation with 355 nm laser radiation, $Tb(Sal)_3Phen$ crystals perceived to be strong white due to the mixing of complementary colors: incident blue photon and green/yellow emission of Tb^{3+} ions [26, 27]. A visual image of as synthesized sample on 355 nm laser excitation is shown in inset (upper right).

It is interesting to note that the emission intensity monitored in case of $Tb(Sal)_3Phen$ complex in PVA film was observed to improve further in presence of Gd^{3+} ion in the complex. It is worth noting that the Gd^{3+} ions are transparent to 355 nm radiation and also to the 415 nm emission of Sal/Phen complex, due to the fact that the lowest excited state of Gd^{3+} ion (~32000 cm^{-1}) is much higher than the triplet states of Sal/Phen. Hence Gd^{3+} ion does not take part directly in the energy transfer to Tb^{3+} ion. It is believed that the presence of additional heavy ion (Gd^{3+}) in the molecular coordination, improves the intersystem crossing (ISC) from singlet manifold to triplet manifold in salicylic anion which provide additional pumping pathway for Tb ions. Additionally it is also expected that as both the rare earth ions (Gd^{3+} and Tb^{3+}) are in the same molecular system, Gd^{3+} ions could act as an energy bridge through which the unabsorbed energy of the Sal/Phen complex in Gd $(Sal)_3Phen$ complex is transferred to Tb^{3+} ions. Hence $Gd(Sal)_3Phen$ complex may act as energy harvesting center and improve the intramolecular energy transfer, which ultimately enhances the emission intensity of Tb^{3+} ions. Similar observations have also been observed in other cases too [28].

Photoluminescence on 310 nm Excitation

Photoluminescence spectra of $TbCl_3$, $Tb(Sal)_3Phen$ and Gd: $Tb(Sal)_3Phen$ complexes doped in PVA film were recorded on 310 nm laser excitation. The 310 nm (~32258 cm^{-1}) laser photon resonates with $^6P_{7/2}$ level (~32051 cm^{-1}) of Gd^{3+} ion and ^7D_j level of Tb^{3+} ion alongwith partial overlapping with $S_0 \rightarrow S_1$ transition of salicylate ligand.

Emission intensity of $TbCl_3$ in PVA film is almost same or less as observed in case of 487 nm excitation, due to the lower extinction at this wavelength. The emission intensity was found to improve further in $Tb(Sal)_3Phen$ complex. Emission spectrum consists of a broad band centered at 415 nm due to salicylate ligand alongwith the usual

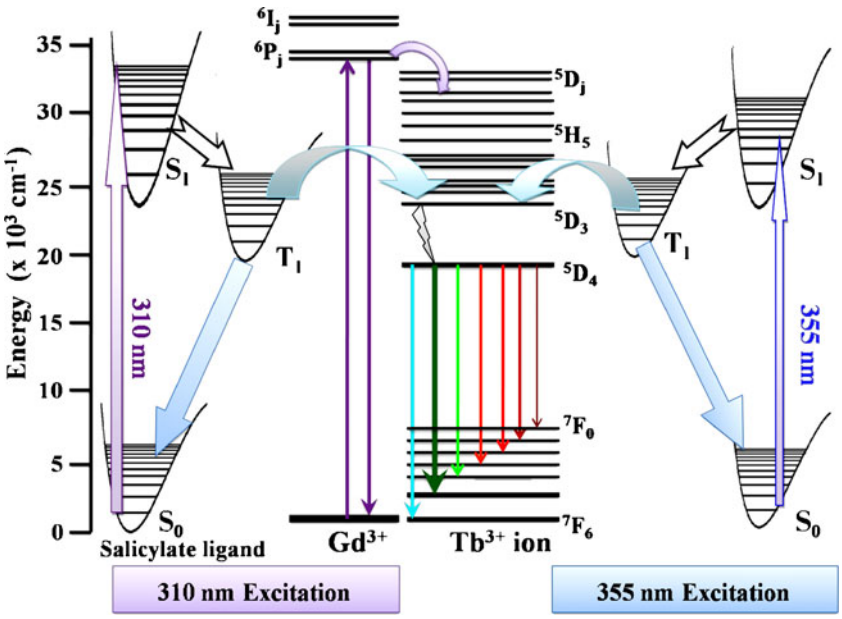

Fig. 7 The schematic energy level diagram explaining the luminescence process and the possible energy transfer pathways for the $Tb(Sal)_3Phen$ complex doped in PVA

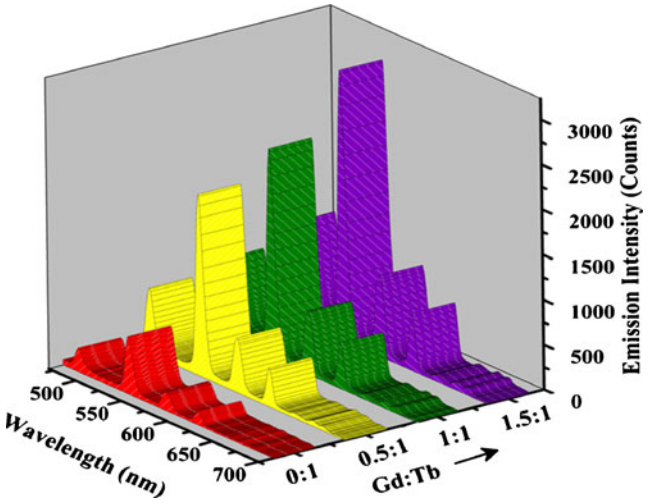

Fig. 8 Variation in Tb^{3+} emission with increasing concentration of Gd^{3+}on 310 nm excitation

characteristic bands of Tb^{3+} ions as observed in previous cases. On excitation with 310 nm photon, salicylate ligand gets excited to S_1 level. Few of the excited electrons in S_1 level depopulate radiatively while the rest were relaxed in T_1 level through intersystem crossing. The enhancement observed in Tb^{3+} emission was due to the intermolecular energy transfer process from triplet state of Sal to Tb^{3+} ions.

Emission intensity of $Gd_{1.0}Tb_{1.0}(Sal)_3Phen$ complex doped in PVA was 8 multiple better compare to $Tb(Sal)_3Phen$ complex, which was improved further with the Gd^{3+} concentration. An increase in percentage of Gd^{3+} in the complex enhances the emission of Tb^{3+} ions showing that energy is transferred non-radiatively to Tb^{3+} ions. The variation in emission intensity of Tb^{3+} with increasing concentration of Gd^{3+} is shown in Fig. 8. First excited level (^6P_j) of Gd^{3+} ion is resonant with 310 nm laser photon and this absorbed energy of Gd^{3+} was transferred non-radiatvely to Tb^{3+} ion through intramolecular energy transfer process. However, no radiative transition of Gd^{3+} ion could be resolved from this laser line.

To validate the aforesaid hypothesis of intramolecular energy transfer, we monitored the photoluminescence spectra of $GdCl_3$ and $Gd_xTb_{1-x}Cl_3$ solution on 266 nm laser excitation. The radiative transitions corresponding to Gd^{3+} ions are very weak in solution so that the variation in emission intensity with respect to Tb^{3+} concentration would not be reliable and within the error estimation. To avoid this problem we recorded the luminescence spectra in crystals of $Gd(Sal)_3Phen$ and $Gd_xTb_{1-x}(Sal)_3Phen$. An intense peak at 310 nm attributed to $^6P_j \rightarrow {}^8S_{7/2}$ transition is observed on 266 nm laser excitation. The 266 nm (~37600 cm^{-1}) laser photon is initially absorbed in ^6I_j manifolds of Gd^{3+} ion and through rapid non-radiative relaxation process it ultimately populates low lying excited ^6P_j levels. Intensity of this band was found to be reciprocal function of Tb^{3+} ion concentration [Fig. 9 (a)]. Subsequent reduction in distance between both the ions leads prevalent energy transfer from Gd^{3+} to Tb^{3+} ions. Due to this energy transfer process the emission intensity of Gd^{3+} ion was suppressed.

Time Resolved Photoluminescence Spectroscopy

Decay curves of $^5D_4 \rightarrow {}^7F_5$ transition of Tb^{3+} ion in its chloride solution and in PVA polymer were recorded at different Tb^{3+} concentrations using pulsed 355 nm laser

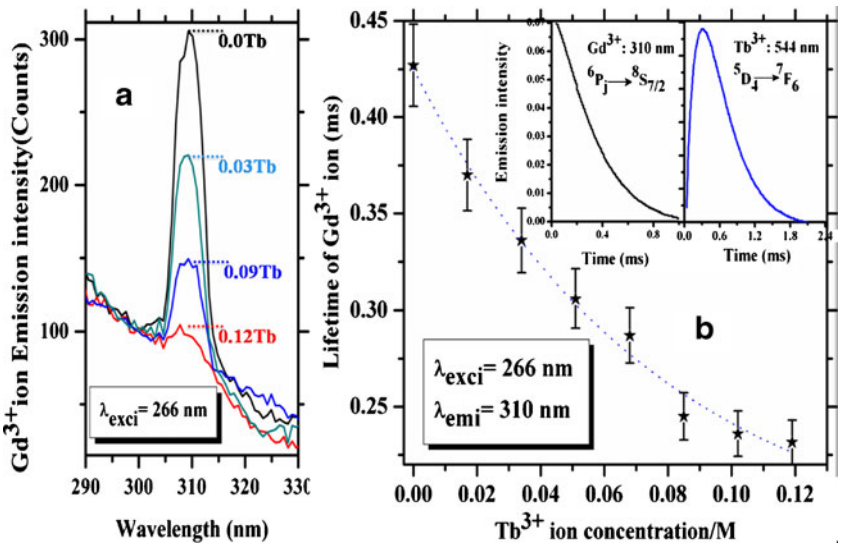

Fig. 9 [**a**] shows variation in emission intensity of Gd ($^6P_j \rightarrow {}^8S_{7/2}$ transition) at 310 nm with Tb ion concentration. [**b**] shows the variation in lifetime of Gd^{3+} ions in solution with respect to Tb^{3+} ion concentration. Inset figures shows the decay curves of $Gd^{3+}$and Tb^{3+} ions for 310 nm and 544 nm emission respectively

Table 1 Variation in risetime (μs) and lifetime (μs) of Tb^{3+} ions corresponding to $^5D_4 \rightarrow {}^5F_5$ (544 nm) transitions (with its different concentration in $GdCl_3$ solution) and lifetime of Gd^{3+} ions for 310 nm ($^6P_J \rightarrow {}^8S_{7/2}$) with concentration fixed at 0.05 M. The energy transfer probability is calculated by using lifetime and relative intensity methods. The last column shows calculated energy transfer efficiency

Tb^{3+} ion (Conc./M)	Lifetime (Tb^{3+}) (μs)	Risetime (Tb^{3+}) (μs)	Lifetime (Gd^{3+}) (μs)	$P_{lifetime}$	$P_{rel.inten.}$	$\eta_{Gd \rightarrow Tb}$
0.0	–	–	450	–	–	–
0.01	385	20.9	378	0.00042	0.00051	0.171
0.03	387	20.7	348	0.00065	0.00072	0.245
0.06	393	19.4	288	0.00125	0.00129	0.360
0.09	397	18.8	255	0.00170	0.00181	0.433
0.12	399	17.4	220	0.00232	0.00241	0.511

radiations. The decay curves were fitted to following exponential function

$$I = I_0\left[A_1 e^{(-t/\tau_1)} + A_2 e^{(-t/\tau_2)}\right] \quad (1)$$

where A_1 and A_2 are the amplitudes, τ_1 and τ_2 are the decaytime and the risetime of the acceptor ion.

The values of τ_1 and τ_2 are found to be ~385 μs and ~20.9 μs, in 0.01 M concentration of Tb^{3+} ions in solution [Table 1]. Initially 355 nm photon is absorbed in $^5L_9$ level of Tb^{3+} ion but emission is solely observed from $^5D_4$ level, relaxing non-radiatively through $^5D_3$ level. The appearance of rise time is due to the slow feeding (slow internal conversion rate) from the $^5D_3$ to $^5D_4$ level. The decay curve of $^5D_4 \rightarrow {}^7F_5$ transition is no more monoexponential beyond 0.12 M concentration (Tb^{3+}) and the lifetime was also reduced considerably. This feature was explained in terms of concentration quenching phenomena [29]. Decay curve of Tb^{3+} ions was slowing down in PVA as compared to the solution of $TbCl_3$ [(solution) 386 μs→430 μs (PVA)]. The increment in lifetime is due to molecular hindrance in PVA sample. In solution most of the energy dissipates through non-radiative relaxation process due to the continuous collisions among Tb^{3+} ions.

Decay curves of $TbCl_3$ and $Tb_{1.0}(Sal)_3Phen$ were plotted on dual logarithmic scale in Fig. 10. The lifetime of $^5D_4$ of Tb^{3+} in $Tb_{1.0}(Sal)_3Phen$ is longer [430 μs→514 μs] than that of $TbCl_3$ showing evidence of energy transfer from Sal/Phen complex to Tb^{3+} ions [30].

The time resolved photoluminescence curves were recorded for Tb^{3+}: $^5D_4 \rightarrow {}^5F_5$ and Gd^{3+}: $^6P_{7/2} \rightarrow {}^8S_{7/2}$ transitions in chloride solution of Gd^{3+} and Tb^{3+} and its crystals. A curve showing the variation in lifetime of Gd^{3+}: $^6P_{7/2} \rightarrow {}^8S_{7/2}$ transition with increase in Tb^{3+} concentration is depicted in Fig. 9b. Keeping in view, the variation in lifetime values we concluded essentially a non-radiative energy transfer process from Gd^{3+} to Tb^{3+}, since the lifetime of Gd^{3+} transition decreases drastically by incorporating Tb^{3+} ions into the solution compared to the case when only Gd^{3+} was present. Photoluminescence intensity of different transitions ($^5D_4 \rightarrow {}^5F_5$ and $^5D_4 \rightarrow {}^5F_6$) of Tb^{3+} ion were recorded as a function of time, keeping Gd^{3+} concentration fixed and tabulated in Table 1. For low concentration of Tb^{3+}, the decay curve was monoexponential, but as the concentration of Tb^{3+} increase beyond 0.12 M, the decay curve gradually deviated from the monoexponential shape showing the involvement of more than one relaxation process [similar to the case of $TbCl_3$ solution]. When the luminescence centers have different local environments, the associated ions relax at different rates. If the rates are dramatically different, the difference in the decay curves would also be easily observed. The reduction in lifetime implies the energy releasing through excited Tb^{3+} ion to unexcited Tb^{3+} ion which quenches the emission intensity. A small risetime of ~20 μs is associated with the decay curve of Tb^{3+} ions even at low concentrations, which reduces further at higher Tb^{3+} concentra-

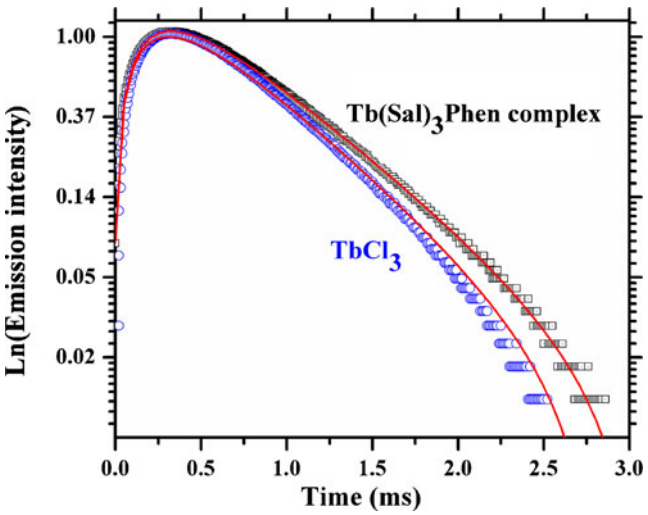

Fig. 10 Decay curves of $TbCl_3$ and $Tb_{1.0}(Sal)_3Phen$ using 355 nm pulsed laser excitation

tions. At higher concentrations ion-ion interaction between two proximate Tb^{3+} ions improved. This strengthened the cross-relaxation process. The fast cross-relaxation process [$^5D_3 \rightarrow {}^5D_4$] appears through reduction in rise time.

Energy transfer probability ($P_{Gd\text{-}Tb}$) can be calculated by two ways in terms of lifetimes and the relative intensity of fluorescence of donor [31, 32] using relation [2] and [3] respectively;

$$P_{D-A} = \frac{1}{\tau_{D-A}} - \frac{1}{\tau_D} \tag{2}$$

$$P_{D-A} = \frac{1}{\tau_D}\left(\frac{I_D}{I_{D-A}} - 1\right) \tag{3}$$

where $I_{D\text{-}A}$,$\tau_{D\text{-}A}$, I_D and τ_D are the fluorescence intensities and lifetime of donor ion in the presence and absence of acceptor ions respectively.

We have calculated the energy transfer efficiencies [Table 1] using the relation given by Joshi et al. [33]

$$E_T = \left(1 - \frac{\tau_{D-A}}{\tau_D}\right) \tag{4}$$

The calculated values of lifetime [$^6P_J \rightarrow {}^8S_{7/2}$ transition], energy transfer probabilities, and efficiencies with respect to the concentration of Tb^{3+} ions are listed in Table 1. A good agreement is seen in the values of energy transfer probability obtained by two methods.

Conclusions

To summarize with $Tb(Sal)_3Phen$ and $Gd{:}Tb(Sal)_3Phen$ complexes doped in PVA were synthesized. Their structural and thermal properties were examined. The luminescent properties of Tb^{3+} ions have been evaluated in its ternary and tertiary complexes by selective excitations. Photoluminescence intensity of Tb^{3+} ions was enhanced when excited with 355 nm laser photon due to the non radiative energy transfer from triplet state of salicylate ligand, which was observed to be further enhanced in presence of Gd^{3+} ions. The enhancement is expected due to the presence of Tb^{3+} and Gd^{3+} ions in the same molecular system. Emission intensity was further improved on excitation with 310 nm due to the dual energy feeding channels [i.e. Sal→Tb and Gd→Tb ions]. Energy transfer parameters viz. transfer probability (using lifetime and relative intensity methods) and energy transfer efficiency have also been calculated.

Acknowledgement Authors are grateful to the AvH foundation, Germany for providing pulsed Nd:YAG laser. One of the authors (Y. Dwivedi) would like to thanks CSIR (India) for Senior Research Fellowship and G. Kaur would like to thanks UGC (India) for Resarch Fellowship in Science for Meritorius Students.

References

1. Svetlana VE, Bunzli JCG (2010) Lanthanide luminescence for functional materials and bio-sciences. Chem Soc Rev 39:189–227
2. Binnemans K (2009) Lanthanide-based luminescent hybrid materials. Chem Rev 109:4283–4374
3. Sun XJ, Li WX, Chai WJ, Ren T, Shi XY (2010) The studies of enhanced fluorescence in the two novel ternary rare-earth complex systems. J Fluoresc 20:453–461
4. An BL, Gong ML, Cheah KW, Wong WK, Zhang JM (2004) Synthesis, structure and photoluminescence of novel lanthanide [(Tb(III), Gd(III)] Complexes with 6-diphenylamine carbonyl 2-pyridine carboxylate. J Alloys Compd 368:326–332
5. Liu G, Jacquier B (2005) Spectroscopic properties of Rare earth in optical materials, Chap. 9. Tsinghua University Press, Springer
6. Li L, Yang J, Wu X, Sun C, Liu Y, Su B (2005) The flourescence enhancement effect of Tb-Gd-adenosine triphosphate-phen system and its analytical application. Atlanta 65:201–205
7. Wang F, Yan B (2008) Intramolecular energy transfer and luminescence enhancement effect in inert rare earth ions (La, Y, Gd)-Eu^{3+}(Tb^{3+}) co fabricated organic-inorganic hybrid materials by covalent grafting. J Photochem Photobiol, A Chem 194:238–246
8. Jiao H, Zhang N, Jing X, Jiao D (2007) Influence of rare earth elements(Sc, La, Gd and Lu) on the luminescent properties of green phosphorY2SiO5:Ce, Tb. Opt Mater 29:1023–1028
9. Yan B, Bai Y-Y (2005) Photophysics of the lanthanide complexes with conjugated carboxylic acids by low temperature fluorescent spectroscopy. J Fluorescence 15:605–611
10. Chen Y, Cai WM (2005) Synthesis and fluorescence properties of rare earth (Eu^{3+} and Gd^{3+}) complexes with α-naphthylacetic acid and 1, 10-phenanthroline. Spectrochim Acta A 62:863–868
11. Levy GC, Lichter RL, Nelson GL (1980) Carbon-13 nuclear magnetic resonance spectroscopy, 2nd edn. Wiley, New York, p 143
12. Nieboer E (1975) Structure and bonding. Springer, Berlin
13. Qiuqing Y, Linshu L (1994) NMR studies of binary and ternary complexes for Eu with 1, 10-phenanthroline and methylbenzoic acid. J Inorg Chem 10:86
14. Yang YT, Zhang SY (2004) Study of lanthanide complexes with salicylic acid by photoacoustic and fluorescence spectroscopy. Spectrochim Acta A 60:2065–2069
15. Wang ZM, He QZ, Yu YH, Luo YQ, Cao JR (2000) Study on the complexes of rare earth with salicylic acid and 1, 10-Phenanthroline. J Shanghai UniV, Nat Sci 29:70–74
16. Xu CJ, Yang H, Xie F, Guo XZ (2005) Photoluminescence enhancement of Sm^{3+} in the Sm^{3+}–salicylic acid–*o*-phenanthroline ternary composite. J Alloys Compd 392:96–99
17. Kim GC, Kim TW, Mho SI, Kim SG, Park HL (1999) Tuning emission colors through cross-relaxation in heavily Tb^{3+} Doped $CaTAlO_4$. J Korean Phys Soc 34:97–99
18. Zhu J, Zhu K, Chen L (2006) Influence of gold nanoparticles on the up-conversion fluorescence in Sm^{3+}. J Non-Cryst Solids 352:150–154
19. Elbanowski M, Makowska B (1996) The lanthanides as luminescent probes in investigations of biochemical systems. J Photochem Photobiol A Chem 99:85–92
20. Weller A (1961) Fast reactions of excited molecules. Progress in reaction kinetics, vol. 1. Pergamon Press, London, p 188

21. Kumar GNH, Rao JL, Gopal NOL, Narasimhulu KV, Chakradhar RPS, Rajulu AV (2004) Spectroscopic investigations of Mn^{2+} ions doped polyvinylalcohol films. Polymer 45:5407–5415
22. Klopfer W (1977) Intramolecular proton transfer in electronically excited molecules. Adv Photochem 10:311–358
23. Bisht PB, Tripathi HB, Pant DD (1995) Cryogenic studies, site selectivity and discrete flourescence in salicylic acid dimer. J Photochem Photobiol A Chem 90:103–108
24. Kaur G, Dwivedi Y, Rai SB (2010) Study of enhanced red emission from $Sm(Sal)_3Phen$ ternary complexes in Poly Vinyl Alcohol film. Opt Comm 283:3441–3447
25. Dwivedi Y, Rai A, Rai SB (2009) Energy transfer in Er:Eu:Yb co-doped tellurite glasses: Yb as enhancer and quencher. J Lumin 129:629–633
26. Dwivedi Y, Rai A, Rai SB (2008) Intense white upconversion emission in Pr/Er/Yb codoped tellurite glass. J Appl Phys 104:043509–043512
27. Dwivedi Y, Kant S, Rai RN, Rai SB (2010) Efficient white light generation from 2,3-diphenyl-1,2-dihydro-quinoxaline complex. Appl Phys B. doi:10.1007/s00340-010-4191-7
28. Sun Y, Zhang W, Wan S, Qingde S (1998) Photoacoustic spectroscopy study on Tb^3 -Gd^3 -Sal complexes. Spectroscopy Let 31:233–241
29. Dwivedi Y, Rai SB (2009) Spectroscopic study of Dy^{3+} and Dy^{3+}/Yb^{3+} ions co-doped in barium fluoroborate glass. Opt Mater 31:1472–1477
30. Zhang RJ, Yang KZ, Yu AC, Zhao XS (2000) Fluorescence lifetime and energy transfer of rare earth β-diketone complexes in organized molecular films. Thin Solid Films 363:275–278
31. Ke HYD, Birnbaum ER (1995) Many-body nonradiative energy transfer in a crystalline europium (III) EDTA complex. J Lumin 63:9–17
32. Braud A, Girard S, Doualan L, Thuau M, Mancorge R, Tkachuk AM (2000) Energy-transfer processes in Yb:Tm-doped KY_3F_{10}, $LiYF_4$, and BaY_2F_8 single crystals for laser operation at 1.5 and 2.3 μm. Phys Rev B 61:5280–5292
33. Joshi BC (1995) Enhanced Eu^{3+} emission by non-radiative energy transfer from Tb^{3+} in Zinc phosphate glass. J Non-Cryst Solids 180:217–220